
White Rose Research Online

eprints@whiterose.ac.uk
https://eprints.whiterose.ac.uk
Universities of Leeds, Sheffield and York

Deposited via The University of Leeds.

White Rose Research Online URL for this paper:
https://eprints.whiterose.ac.uk/id/eprint/171119/

Version: Supplemental Material

Article:
Lord, RM, Zegke, M, Basri, AM et al. (2021) Rhodium(III) Dihalido Complexes: The Effect of Ligand Substitution and Halido Coordination on Increasing Cancer Cell Potency. Inorganic Chemistry, 60 (3). pp. 2076-2086. ISSN: 0020-1669

https://doi.org/10.1021/acs.inorgchem.0c03704

© 2021 American Chemical Society. This is an author produced version of an article, published in Inorganic Chemistry. Uploaded in accordance with the publisher's self-archiving policy.

Reuse
Items deposited in White Rose Research Online are protected by copyright, with all rights reserved unless indicated otherwise. They may be downloaded and/or printed for private study, or other acts as permitted by national copyright laws. The publisher or other rights holders may allow further reproduction and re-use of the full text version. This is indicated by the licence information on the White Rose Research Online record for the item.

Takedown
If you consider content in White Rose Research Online to be in breach of UK law, please notify us by emailing eprints@whiterose.ac.uk including the URL of the record and the reason for the withdrawal request.



Rhodium(III) dihalido complexes: the effect of ligand substitution and halido coordination on increasing cancer cell potency

Rianne M. Lord,[a,b]* Markus Zegke,[b] Aida M. Basri,[c] Christopher M. Pask[c] and Patrick C. McGowan[c]

[a] School of Chemistry, University of East Anglia, Norwich Research Park, Norwich, NR4 7TJ, U.K. Email: r.lord@uea.ac.uk

[b] School of Chemistry and Biosciences, University of Bradford, Bradford, BD7 1DP, U.K.

[c] School of Chemistry, University of Leeds, Woodhouse Lane, Leeds, LS2 9JT, U.K.

X-ray Crystallographic Analysis

Table S 1 X-ray crystallographic data for complexes **1**, **3 (Δ and Λ)**, **4a** and **4b**, s.u.s shown in parenthesis

Complex	1	3 (Δ)	3 (Λ)	4a	4b
CCDC Number	1978080	1978078	2042715	1978082	1978081
Empirical formula	$C_{25}H_{21}Cl_2F_2N_4O_3Rh$	$C_{24}H_{17}Br_2Cl_2N_4O_2Rh$	$C_{24}H_{17}Br_2Cl_2N_4O_2Rh$	$C_{26}H_{25}Cl_2I_2N_4O_4Rh$	$C_{27}H_{24}Cl_2I_2N_5O_3Rh$
Formula weight	637.278	727.046	727.046	885.132	894.143
Temperature/K	100.1(4)	99.9(3)	100.3(9)	100.2(4)	120.3(7)
Crystal system	orthorhombic	monoclinic	monoclinic	monoclinic	monoclinic
Space group	$P2_12_12_1$	Cc	Cc	$P2_1/c$	$P2_1/n$
a/Å	10.5456(3)	9.3613(3)	9.3527(2)	17.9801(8)	8.1441(3)
b/Å	12.0060(4)	23.8677(7)	23.9723(6)	10.3200(4)	32.8058(12)
c/Å	19.5775(7)	11.4997(3)	11.5084(3)	17.7408(9)	11.0381(4)
α/°	90	90	90	90	90
β/°	90	100.495(3)	100.627(2)	115.036(6)	90.522(3)
γ/°	90	90	90	90	90
Volume/Å³	2478.72(14)	2526.43(13)	2535.99(11)	2982.6(3)	2948.98(18)
Z	4	4	4	4	4
ρ_{calc}g/cm³	1.708	1.911	1.904	1.971	2.014
μ/mm⁻¹	0.956	4.081	4.065	2.860	23.116
F(000)	1277.3	1411.6	1411.6	1698.2	1729.4
Crystal size/mm³	0.478 × 0.202 × 0.132	0.093 × 0.06 × 0.04	0.21 x 0.15 x 0.09	0.412 × 0.366 × 0.316	0.102 × 0.072 × 0.035
Radiation	Mo Kα (λ = 0.71073)	Mo Kα (λ = 0.71073)	Mo Kα (λ = 0.71073	Mo Kα (λ = 0.71073)	Cu Kα (λ = 1.54184)
2Θ range for data collection/°	6.62 to 59.08	6.42 to 51.36	4.74 to 60.72	6.38 to 59.06	8.46 to 147.42
Index ranges	-14 ≤ h ≤ 10, -15 ≤ k ≤ 15, -19 ≤ l ≤ 27	-8 ≤ h ≤ 11, -25 ≤ k ≤ 28, -14 ≤ l ≤ 14	-11 ≤ h ≤ 12, -23 ≤ k ≤ 31, -14 ≤ l ≤ 12	-24 ≤ h ≤ 20, -13 ≤ k ≤ 14, -24 ≤ l ≤ 24	-9 ≤ h ≤ 9, -38 ≤ k ≤ 40, -13 ≤ l ≤ 13
Reflections collected	9366	6634	6999	19498	13120
Independent reflections	5515 [R_{int} = 0.0438, R_{sigma} = 0.0893]	3782 [R_{int} = 0.0263, R_{sigma} = 0.0397]	5022 [R_{int} = 0.0176, R_{sigma} = 0.0299]	7240 [R_{int} = 0.0499, R_{sigma} = 0.0645]	5776 [R_{int} = 0.0571, R_{sigma} = 0.0721]
Data/restraints/parameters	5515/0/336	3782/2/316	5022/2/316	7240/0/356	5776/0/363
Goodness-of-fit on F²	1.040	1.047	1.022	1.051	1.064
Final R indexes [I>=2σ (I)]	R_1 = 0.0524, wR_2 = 0.1092	R_1 = 0.0228, wR_2 = 0.0513	R_1 = 0.0243, wR_2 = 0.0614	R_1 = 0.0499, wR_2 = 0.0972	R_1 = 0.0565, wR_2 = 0.1339
Final R indexes [all data]	R_1 = 0.0636, wR_2 = 0.1170	R_1 = 0.0238, wR_2 = 0.0519	R_1 = 0.0258, wR_2 = 0.0619	R_1 = 0.0668, wR_2 = 0.1063	R_1 = 0.0707, wR_2 = 0.1438
Largest diff. peak/hole / e Å⁻³	1.38/-0.90	0.47/-0.35	0.78/-0.45	3.04/-2.54	2.14/-1.50
Flack parameter	-0.07(5)	0.017(6)	0.025(5)	--	--

Table S 2 Selected bond angles (°) for complexes **1**, **3 (Δ and Λ)**, **4a** and **4b**, s.u.s shown in parentheses

Bonds	1	3 (Δ)	3 (Λ)	4a	4b
X(1)-Rh(1)-X(2)	92.33(7)	93.00(4)	92.93(3)	90.86(5)	177.88(7)
X(1)-Rh(1)-O(2)	177.09(15)	177.14(8)	177.19(7)	176.28(11)	86.76(16)
X(2)-Rh(1)-O(2)	88.46(13)	86.00(8)	86.09(7)	91.14(11)	91.98(16)
X(1)-Rh(1)-N(1)	89.41(17)	89.02(10)	89.25(9)	89.18(12)	175.3(2)
X(2)-Rh(1)-N(1)	96.79(18)	96.06(10)	96.06(9)	95.31(13)	88.28(18)
X(1)-Rh(1)-N(2)	90.46(18)	90.32(10)	90.50(9)	89.48(13)	90.58(19)
X(2)-Rh(1)-N(2)	175.70(18)	175.11(9)	175.10(9)	175.45(12)	90.60(19)
X(1)-Rh(1)-N(3)	96.85(19)	97.62(10)	97.66(9)	96.48(13)	92.26(18)
X(2)-Rh(1)-N(3)	88.75(17)	86.14(10)	86.09(9)	88.26(13)	89.16(18)
N(1)-Rh(1)-O(2)	93.3(2)	93.74(12)	93.47(11)	93.75(15)	97.7(2)
N(2)-Rh(1)-O(2)	88.9(2)	90.85(13)	90.65(11)	88.78(16)	176.3(3)
N(3)-Rh(1)-O(2)	80.4(2)	79.65(12)	79.66(11)	80.45(15)	78.4(2)
N(1)-Rh(2)-N(2)	80.0(2)	80.40(14)	80.48(12)	80.16(17)	79.7(3)
N(1)-Rh(1)-N(3)	171.5(2)	172.90(13)	172.67(12)	173.27(17)	175.3(2)
N(2)-Rh(1)-N(3)	94.2(2)	96.98(13)	96.92(12)	96.21(17)	104.3(3)

Table S 3 X-ray crystallographic data for complexes **6** and **7**, s.u.s shown in parenthesis

Complex	6	7
CCDC Number	1978079	1978083
Empirical formula	$C_{27}H_{24}Cl_2I_2N_5O_3Rh$	$C_{27}H_{24}Br_2I_2N_5O_3Rh$
Formula weight	894.143	983.045
Temperature/K	100.0(3)	120.2(4)
Crystal system	monoclinic	monoclinic
Space group	Cc	Cc
a/Å	15.4740(11)	15.5643(6)
b/Å	9.1361(6)	9.1945(4)
c/Å	21.4115(13)	21.4844(10)
α/°	90	90
β/°	95.700(6)	95.650(4)
γ/°	90	90
Volume/Å^3	3012.0(4)	3059.6(2)
Z	4	4
ρ_{calc}g/cm^3	1.972	2.134
μ/mm^{-1}	2.832	5.225
F(000)	1714.2	1855.4
Crystal size/mm^3	0.118 × 0.108 × 0.031	0.15 × 0.09 × 0.07
Radiation	Mo Kα (λ = 0.71073)	Mo Kα (λ = 0.71073)
2Θ range for data collection/°	6.22 to 52.74	6.18 to 62.3
Index ranges	-16 ≤ h ≤ 19, -11 ≤ k ≤ 9, -26 ≤ l ≤ 21	-21 ≤ h ≤ 22, -11 ≤ k ≤ 12, -22 ≤ l ≤ 28
Reflections collected	9196	10526
Independent reflections	4805 [R_{int} = 0.0675, R_{sigma} = 0.1033]	6153 [R_{int} = 0.0368, R_{sigma} = 0.0602]
Data/restraints/parameters	4805/98/309	6153/2/363
Goodness-of-fit on F^2	1.052	1.018
Final R indexes [I>=2σ (I)]	R_1 = 0.0512, wR_2 = 0.0906	R_1 = 0.0383, wR_2 = 0.0806
Final R indexes [all data]	R_1 = 0.0675, wR_2 = 0.1016	R_1 = 0.0432, wR_2 = 0.0840
Largest diff. peak/hole / e Å^{-3}	1.01/-0.91	1.00/-0.77
Flack parameter	-0.06(4)	0.040(12)

Table S 4 Selected bond angles (°) for complexes **6** and **7**, s.u.s shown in parentheses

Bonds	6	7
X(1)-Rh(1)-X(2)	177.34(5)	174.38(2)
X(1)-Rh(1)-O(2)	88.1(2)	88.21(14)
X(2)-Rh(1)-O(2)	89.4(2)	86.66(14)
X(1)-Rh(1)-N(1)	89.9(3)	89.13(16)
X(2)-Rh(1)-N(1)	89.5(3)	89.20(14)
X(1)-Rh(1)-N(2)	92.4(3)	91.31(16)
X(2)-Rh(1)-N(2)	90.0(3)	93.63(16)
X(1)-Rh(1)-N(3)	88.4(3)	92.10(15)
X(2)-Rh(1)-N(3)	91.9(3)	89.01(145
N(1)-Rh(1)-O(2)	94.9(4)	96.8(2)
N(2)-Rh(1)-O(2)	174.9(4)	175.7(2)
N(3)-Rh(1)-O(2)	78.2(3)	77.3(2)
N(1)-Rh(2)-N(2)	80.0(4)	79.0(2)
N(1)-Rh(1)-N(3)	173.0(4)	173.9(2)
N(2)-Rh(1)-N(3)	106.7(5)	107.0(2)

Characterization by FTIR and PXRD

FTIR Spectroscopy for Complex 3 Isomers

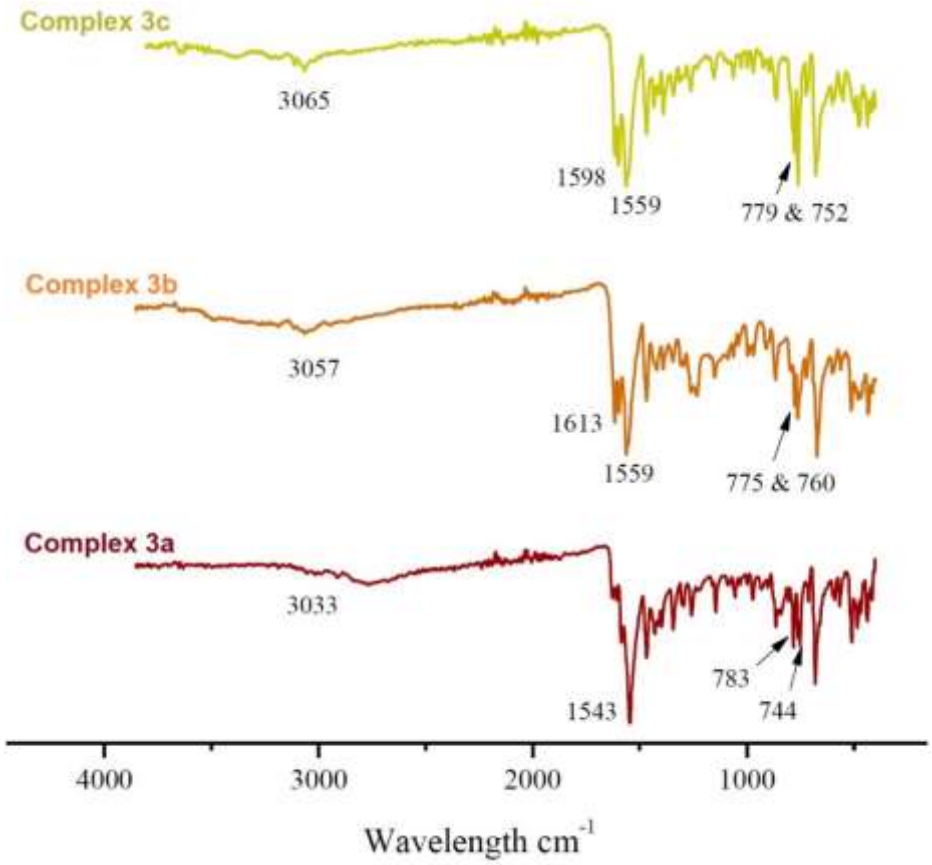

Figure S 1 IR spectra of complexes **3a** (**red**), **3b** (**orange**) and **3c** (**yellow**).

PXRD of Complexes 3 and Complex 7

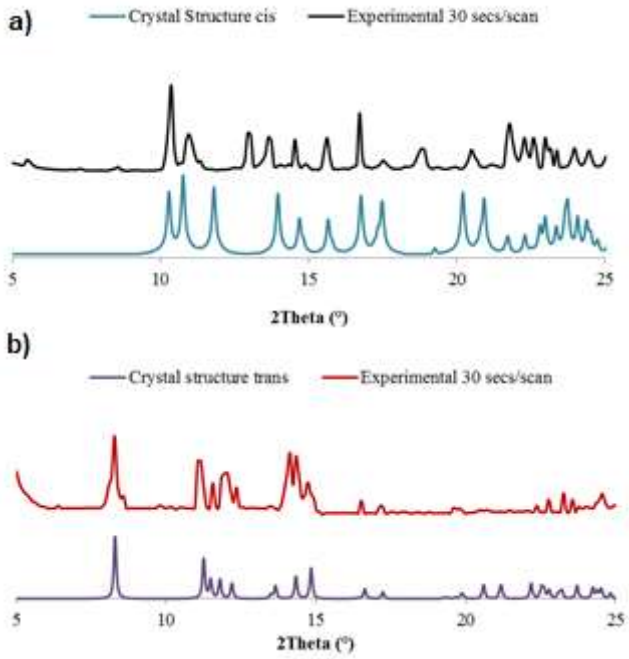

Figure S 2 Simulated and experimental PXRD diffractograms for **a)** complex **3** and **b)** complex **7**.

Characterization NMR Spectroscopy

Complex 3 – 1st synthetic products

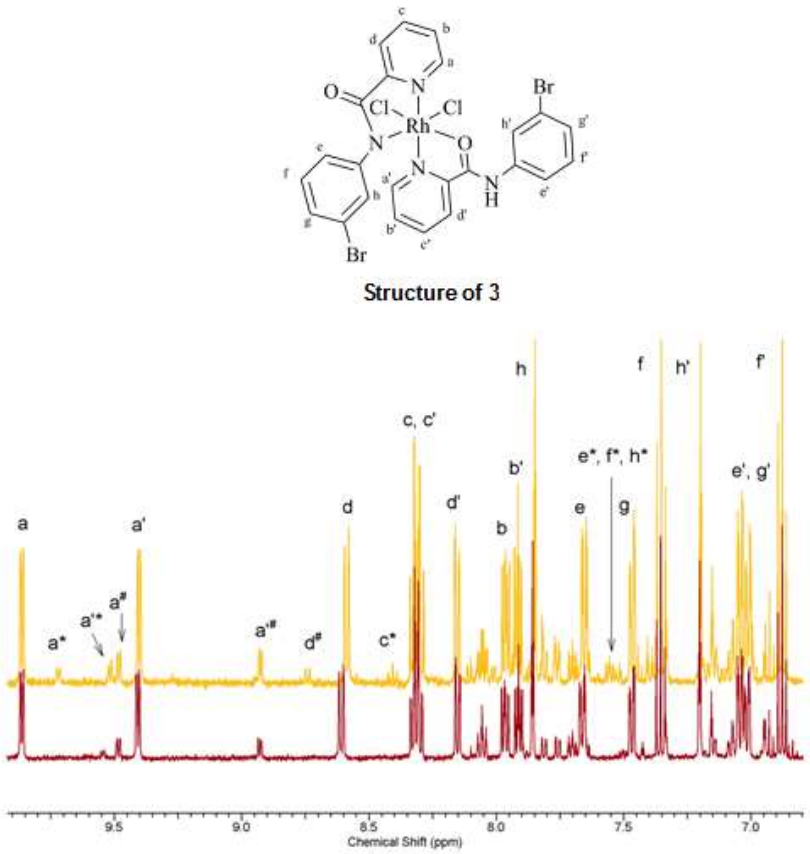

Figure S 3 ^{1}H NMR spectra of complexes **3a** (**red**) and **3c** (**yellow**) (d_6-acetone, 300 K, 300 MHz).

Variable Temperature NMR Spectroscopy of Complex 3 – 1st synthetic product

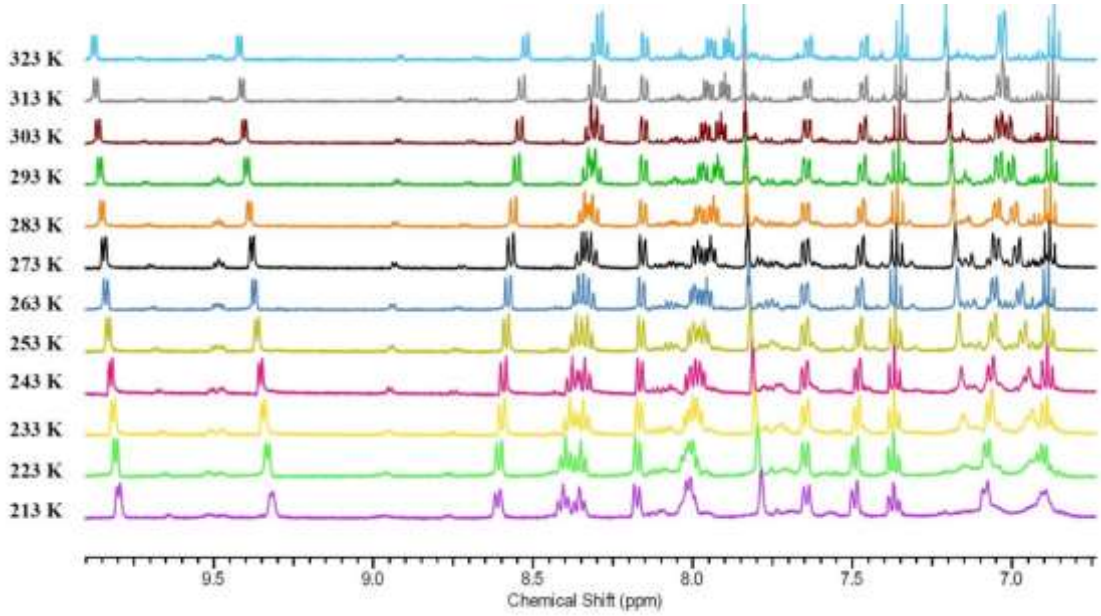

Figure S 4 Temperature-dependent ^{1}H NMR spectra of complex **3c** (d_6-acetone, 300 K, 300 MHz).

NMR for Complex 3 – 2nd synthetic product

Figure S 5 Image of the combined crystals under a microscope

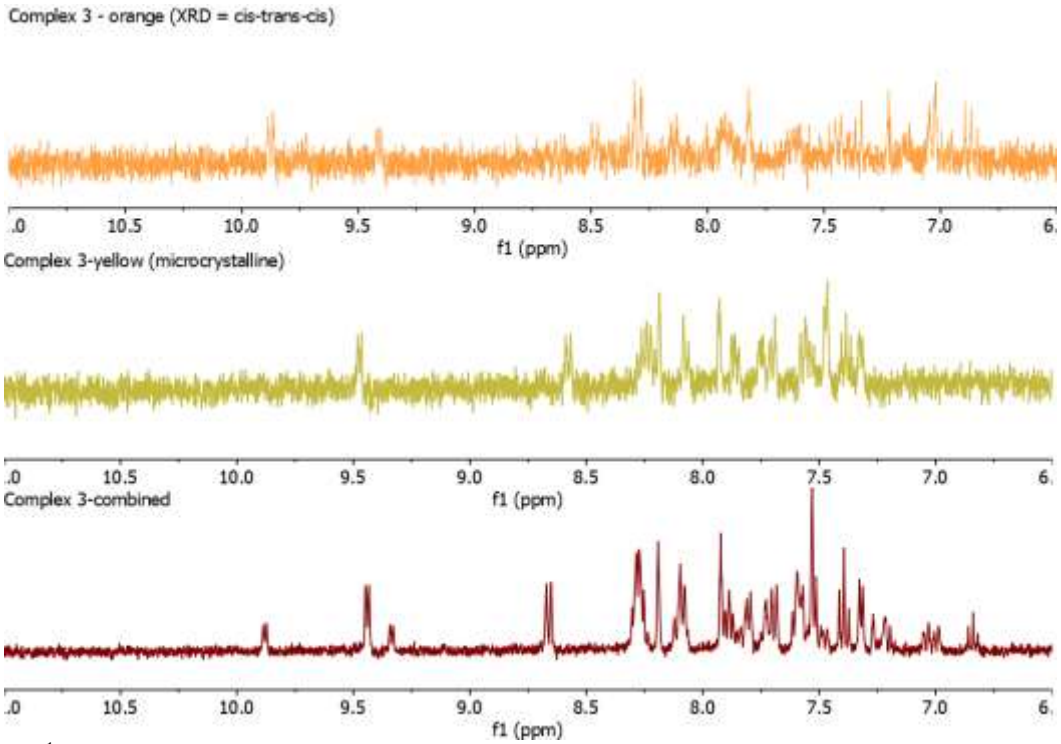

Figure S 6 ^{1}H NMR spectra of complexes **3-combined** (**red**) and **3-yellow microcrystals** and **3-orange single crystals** (d_6-acetone, 300 K, 400 MHz).

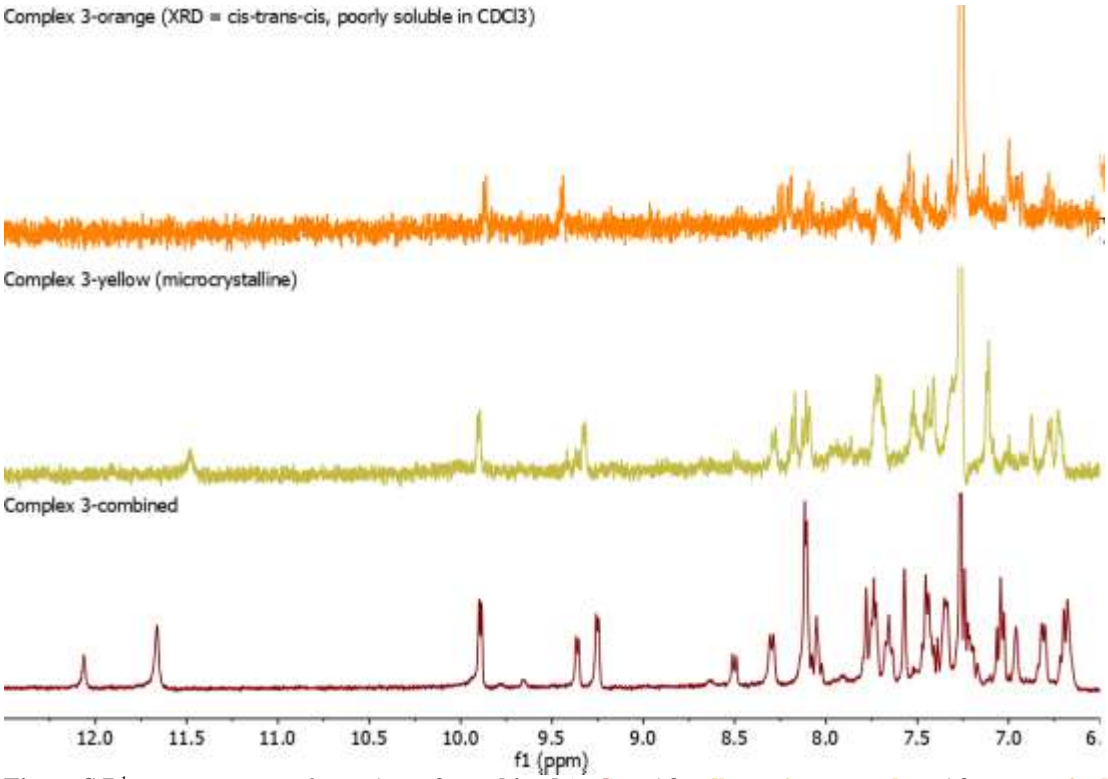

Figure S 7 ^{1}H NMR spectra of complexes **3-combined** (**red**) and **3-yellow microcrystals** and **3-orange single crystals** (CDC_3, 300 K, 400 MHz).

NMR Characterisation and Exchange Studies of Complexes 1, 4, 5 and 8

Comparison NMR spectroscopy of complexes 1 and 5

^{1}H NMR spectra were recorded for **[(3'-F)(3'-FH)RhCl$_2$]** (**1**, **black**) and **[(3'-F)(3'-FH)RhI$_2$]** (**5**, **blue**) (**Figure S4**) at room temperature and show that complex **1** exhibits multiple isomers in solution, whereas complex **5** has only one isomer in solution. This can be clearly observed for the NH proton of the ligand, which appears at a chemical shift of ~12.5 ppm.

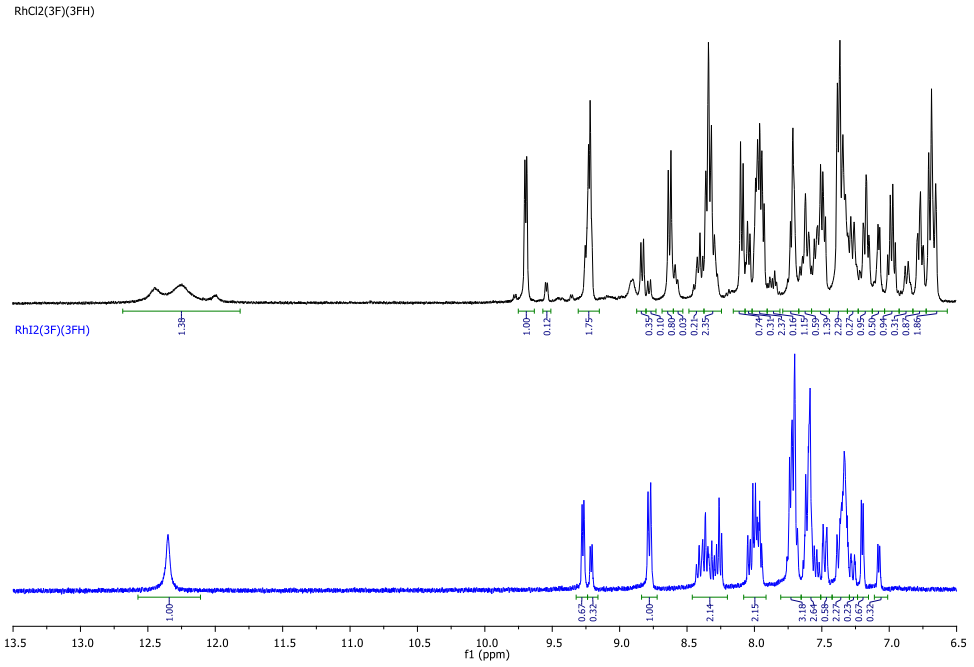

Figure S 8 ^{1}H NMR spectrum of **[(3'-F)(3'-FH)RhCl$_2$]** (**1**, **black**) and **[(3'-F)(3'-FH)RhI$_2$]** (**5**, **blue**) confirming the different number of isomer present ($CDCl_3$, 300 K, 400 MHz)

NMR's in Chloroform

Complex 1 + N-(3-iodophenyl)picolinamide

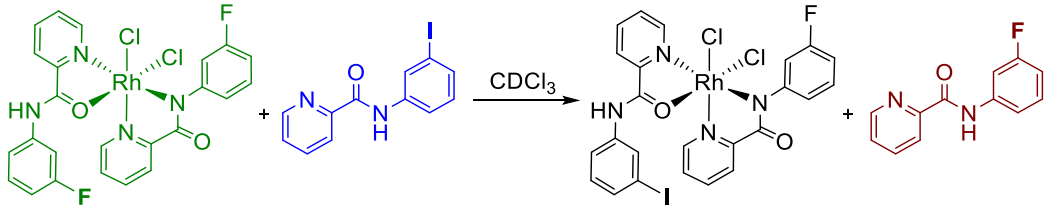

Scheme S1 Ligand exchange of **[(3'-F)(3'-FH)RhCl$_2$]** (**1**) with ligand **3'-IH** in $CDCl_3$.

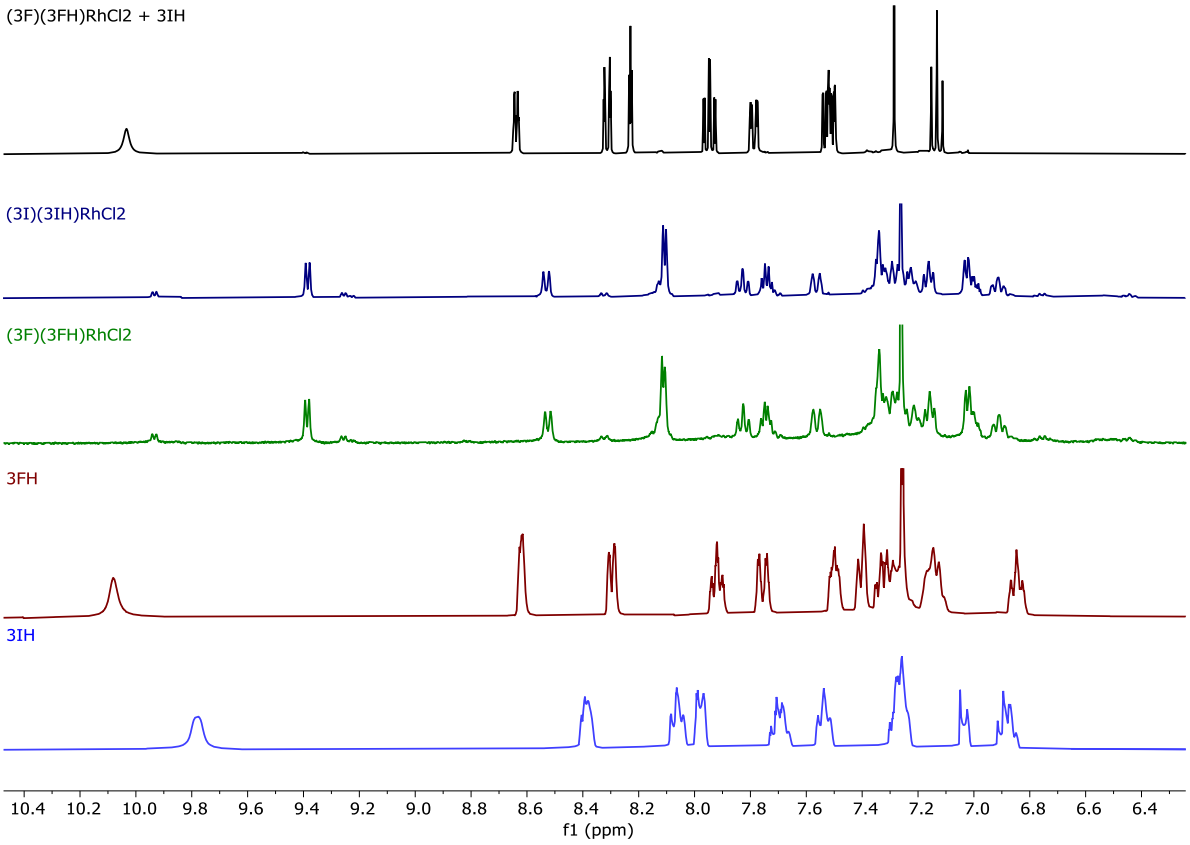

Figure S 9 Overlay of the product (**black**) from the reaction of **[(3'-F)(3'-FH)RhCl$_2$]** (**1**, **dark green**) + ligand **3'-IH** (**blue**). The spectra for **[(3'-I)(3'-IH)RhCl$_2$]** (**4**, **dark blue**) and ligand **3'-FH** (**dark red**) are also included for comparison ($CDCl_3$, 300 K, 400 MHz).

The ^{1}H NMR study of an equimolar mixture of **[(3'-F)(3'-FH)RhCl$_2$] (1)** and ***N*-(3-iodophenyl)picolinamide (3'-IH)** in $CDCl_3$ shows the formation of a mixed species which is possibly **[(3'-F)(3'-IH)RhCl$_2$] or [(3'-FH)(3'-I)RhCl$_2$]** and the dissociation of ***N*-(3-fluorophenyl)picolinamide (3'-FH)**. The resonances of [(3'-L)(3'-LH)RhCl$_2$] are "swamped" by the free ligand due to the complex's poor solubility in $CDCl_3$. In addition, the ^{1}H NMR spectra of **[(3'-F)(3'-FH)RhCl$_2$] (1)** and **[(3'-I)(3'-IH)RhCl$_2$] (4)** are essentially indistinguishable, thus inhibiting a direct *in situ* analysis of a mixed **[(3'-F)(3'-IH)RhCl$_2$] or [(3'-FH)(3'-I)RhCl$_2$]** complex.

Complex 4 + N-(3-fluorophenyl)picolinamide

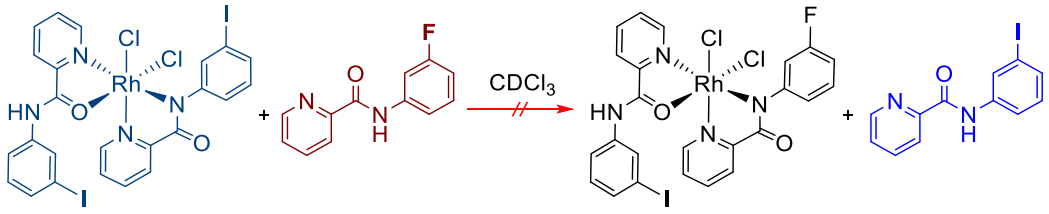

Scheme S2 Attempted ligand exchange of **[(3'-I)(3'-IH)RhCl$_2$]** (**4**) with **3'-FH** in $CDCl_3$.

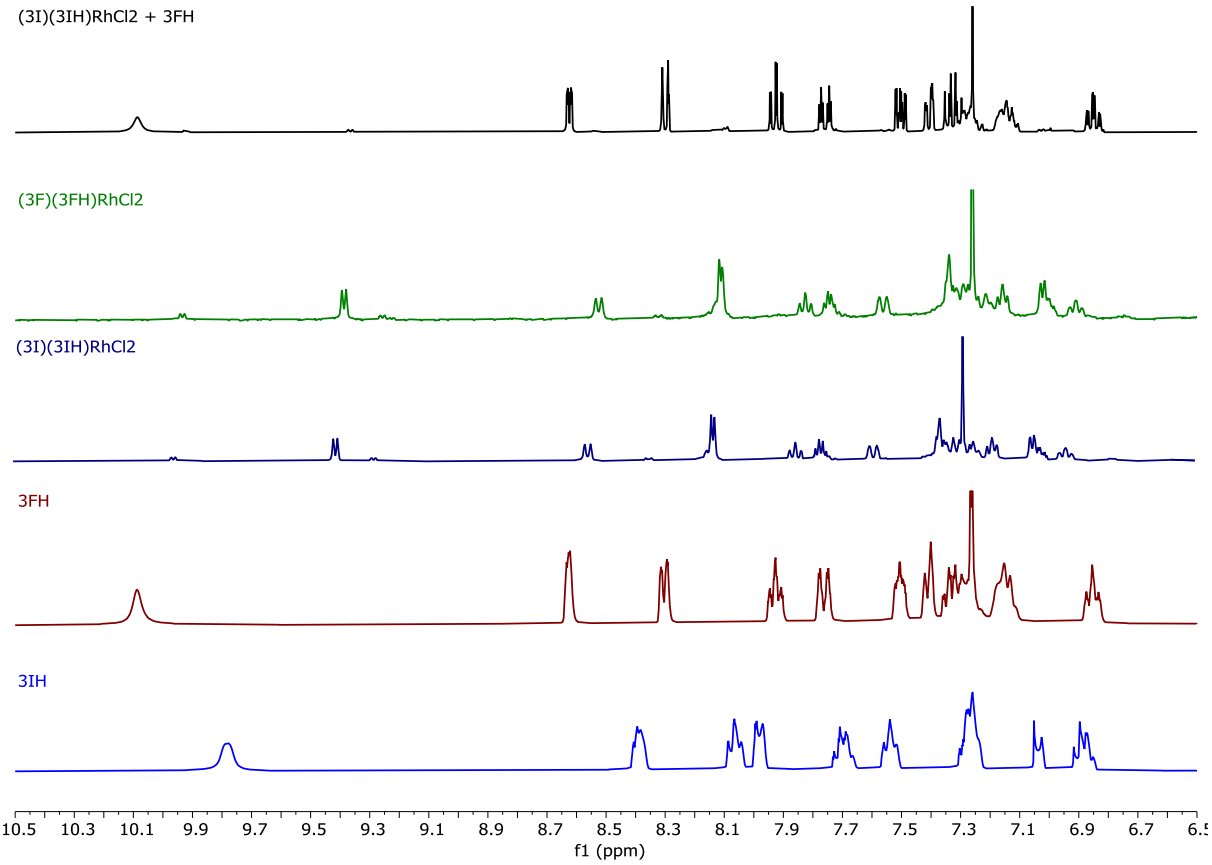

Figure S 10 Overlay of the product (**black**) from the reaction of **[(3'-I)(3'-IH)RhCl$_2$]** (**4**, **dark blue**) + 3'-FH (**dark red**). The spectra for **[(3'-F)(3'-FH)RhCl$_2$]** (**1**, **dark green**) and **3'-IH** (**blue**) are also included for comparison ($CDCl_3$, 300 K, 400 MHz).

The ^{1}H NMR study of an equimolar mixture of **[(3'-I)(3'-IH)RhCl$_2$] (4)** and ***N*-(3-fluorophenyl)picolinamide (3'-IH)** in $CDCl_3$ confirms that the ***N*-(3-fluorophenyl)picolinamide** is the ligand which is most easily substituted, and that the formation of the complex **[(3'-I)(3'-IH)RhCl$_2$] (4)** is energetically favoured. The spectrum of the mixture shows essentially only the resonances of the added ***N*-(3-fluorophenyl)picolinamide** ligand, as the resonances of [(3'-X)(3'-XH)RhCl$_2$] are again "swamped" by the free ligand due to the complex's poor solubility in $CDCl_3$. No resonances of liberated ***N*-(3-fluorophenyl)picolinamide** can be observed.

Complex 5 + N-(3-iodophenyl)picolinamide

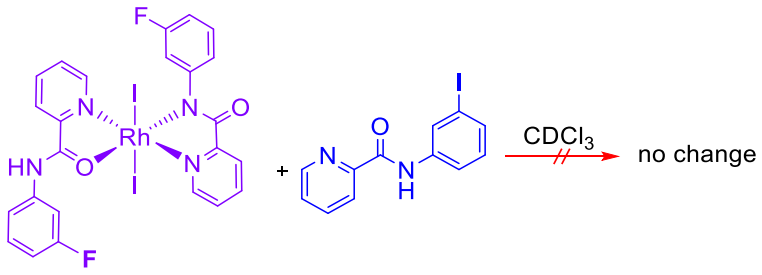

Scheme S3 Test reaction for the ligand exchange between **[(3'-F)(3'-FH)RhI$_2$]** (**5**) with **3'-IH** in $CDCl_3$.

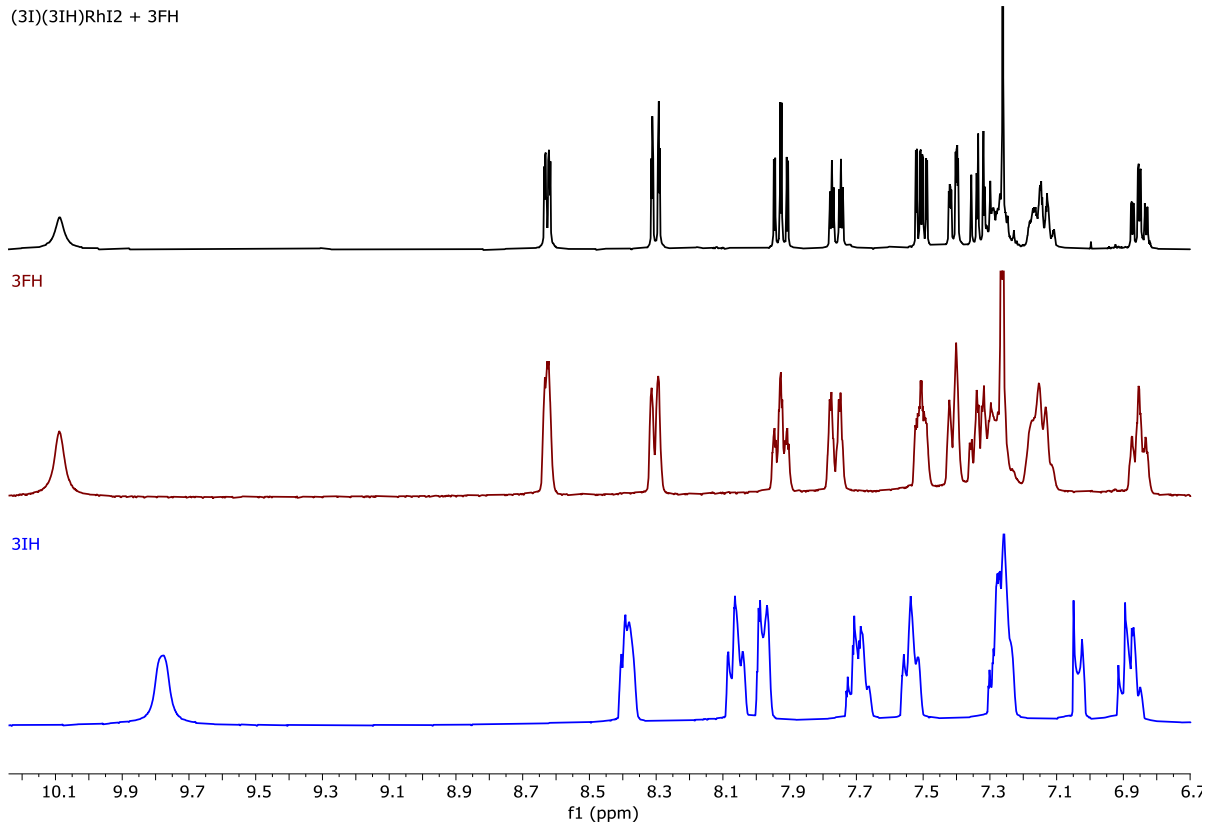

Figure S 11 Overlay of the product (**black**) from the reaction of **[(3'-F)(3'-FH)RhI2]** (**5**) + **3'-IH** (**blue**) The spectra for ligand **3'-FH** (**dark red**) is also included for comparison ($CDCl_3$, 300 K, 400 MHz).

The ^{1}H-NMR study of an equimolar mixture of **[(3'-F)(3'-FH)RhI$_2$]** (**5**) and ***N*-(3-iodophenyl)picolinamide (3'-IH)** in $CDCl_3$ shows free **3'-IH** exclusively. No ligand exchange can be observed as no resonances of liberated ***N*-(3-fluorophenyl)picolinamide (3'-FH)** are present. The extremely poor solubility of **[(3'-F)(3'-FH)RhI$_2$]** in $CDCl_3$ does not allow for a direct comparison of **[(3'-F)(3'-FH)RhI$_2$]** (**5**) and **[(3'-I)(3'-IH)RhI$_2$]** (**8**) and a mixed complex **[(3'-F)(3'-IH)RhI$_2$]** in this solvent. Therefore, the spectra for complex **[(3'-I)(3'-IH)RhI$_2$]** (**8**) + **3'-FH** was not recorded.

NMR's in Dimethyl sulfoxide

Complex 1 + N-(3-iodophenyl)picolinamide

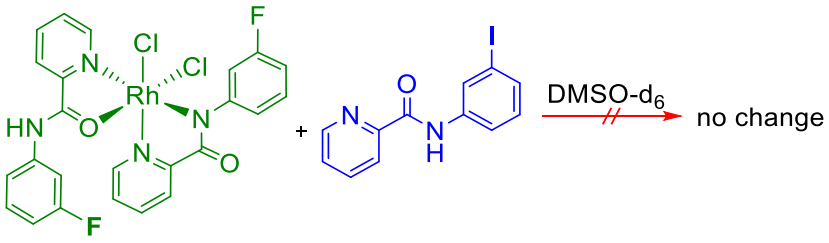

Scheme S4 Test reaction for the ligand exchange between **[(3'-F)(3'-FH)RhCl$_2$]** (**1**) with **3'-IH** in d$_6$-DMSO.

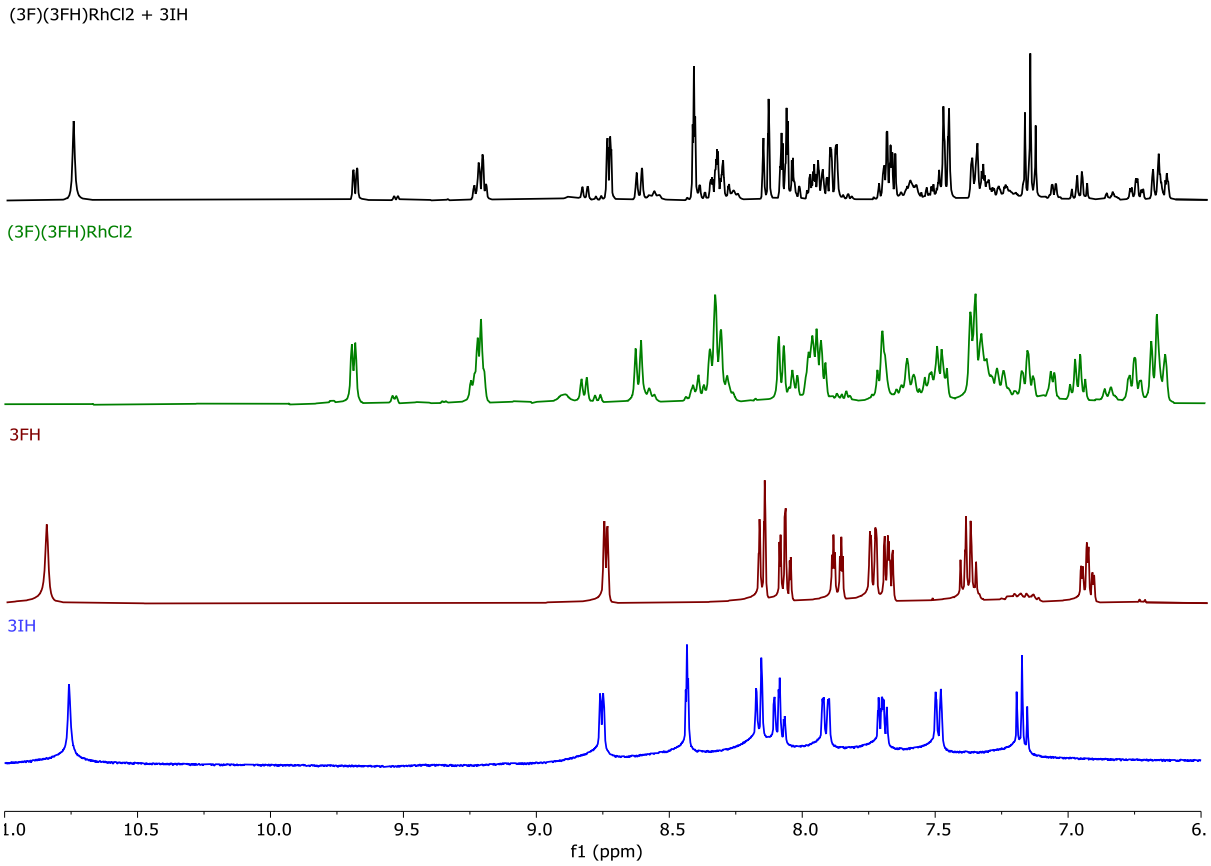

Figure S 12 Overlay of the product (**black**) from the reaction of **[(3'-F)(3'-FH)RhCl$_2$]** (**1**, **dark green**) + **3'-IH** (**blue**). The spectra for ligand **3'-FH** (**dark red**) is also included for comparison (d$_6$-DMSO, 300 K, 400 MHz).

The ^{1}H-NMR study of an equimolar mixture of **[(3'-F)(3'-FH)RhCl$_2$] (1)** and ***N*-(3-iodophenyl)picolinamide (3'-IH)** in d$_6$-DMSO shows no changes in the resonances of the starting material and only an additional set of resonances for the free **3'-IH**. No resonances of free **3'-FH** can be observed, indicating no ligand exchange for **[(3'-L)(3'-LH)RhCl$_2$]** complexes in DMSO.

Complex 5 + N-(3-iodophenyl)picolinamide

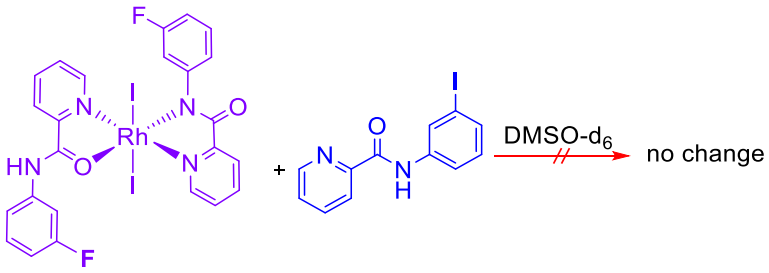

Scheme S5 Test reaction for the ligand exchange between **[(3'-F)(3'-FH)RhI$_2$]** (**5**) with **3'-IH** in d$_6$-DMSO.

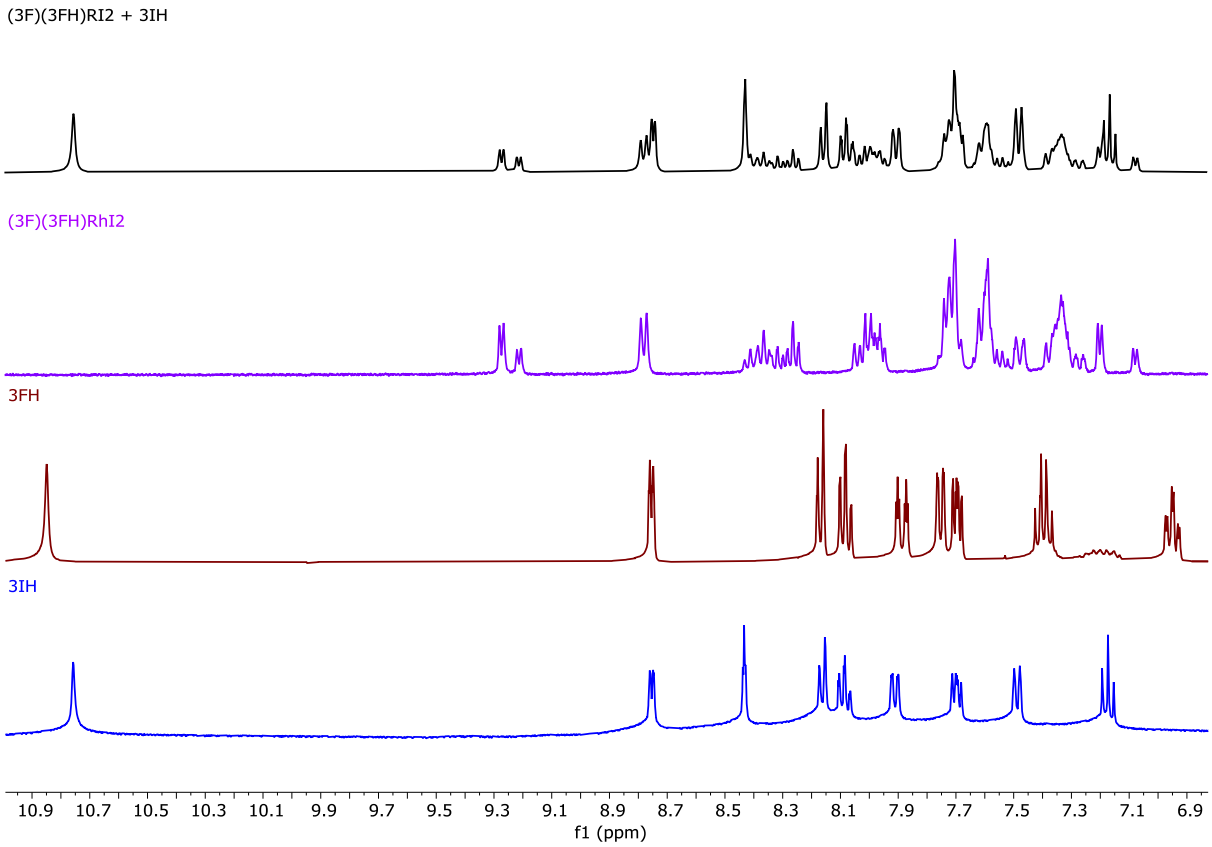

Figure S 13 Overlay of the product (**black**) from the reaction of **[(3'-F)(3'-FH)RhI2]** (**5**) + **3'-IH** (**blue**) The spectra for ligand **3'-FH** (**dark red**) is also included for comparison (d$_6$-DMSO, 300 K, 400 MHz).

The ^{1}H-NMR study of an equimolar mixture of **[(3'-F)(3'-FH)RhI$_2$] (5)** and ***N*-(3-iodophenyl)picolinamide (3'-IH)** in d$_6$-DMSO confirms that complexes of the type **[(3'-L)(3'-LH)RhI$_2$]** do not undergo ligand exchange in DMSO. Along with the resonances of the starting material an additional set of resonances for the free **3'-IH** can be seen, with no resonances of free **3'-FH**, further indicating a lack of ligand exchange in solution.

Stability and Ligand Exchange Studies of Complex 3 and 7 over 96 h

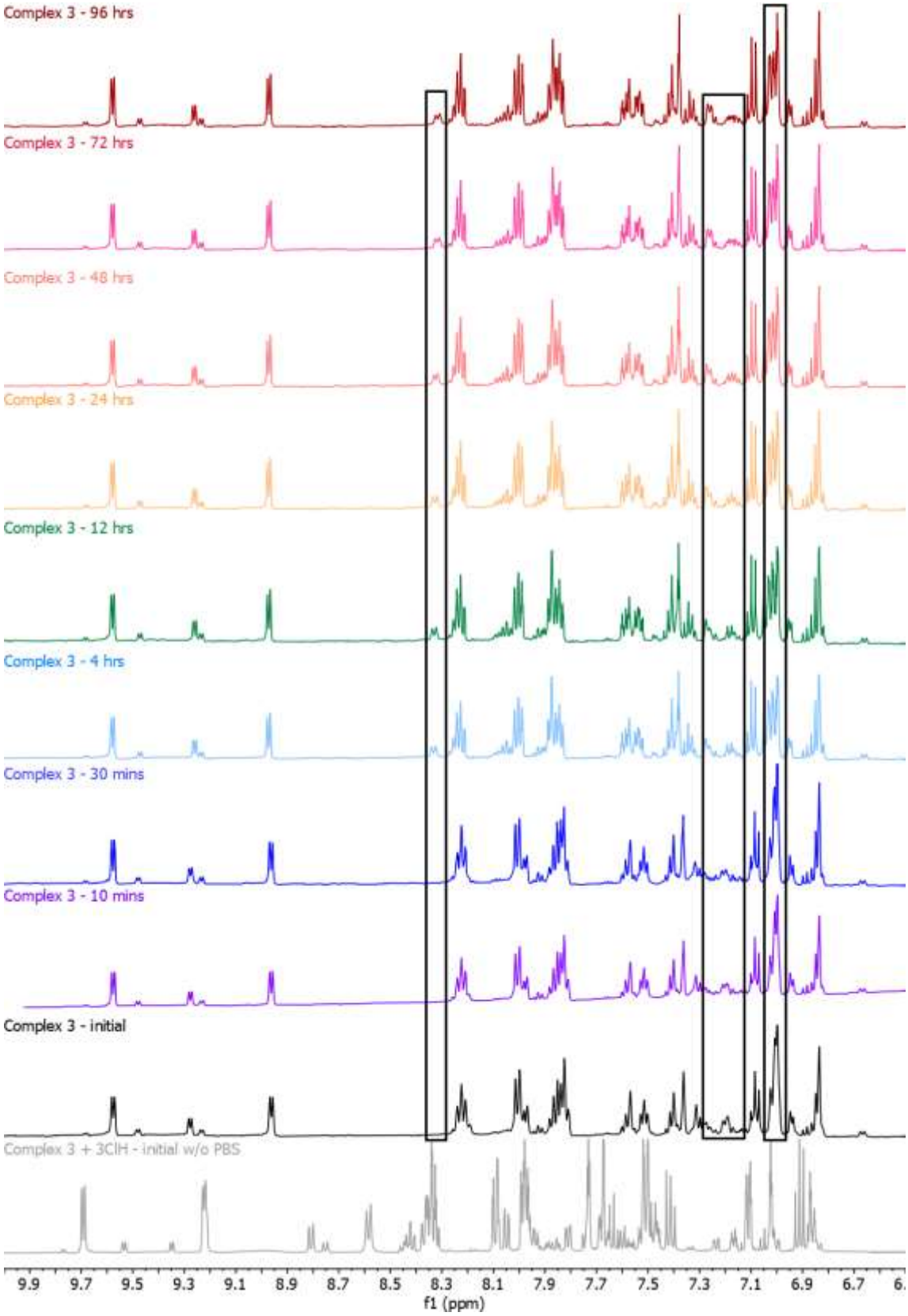

Figure S 14 Stability study of complex **3** in DMSO:PBS (80:20 v/v) over 96 h (d_6-DMSO, 300 K, 400 MHz).

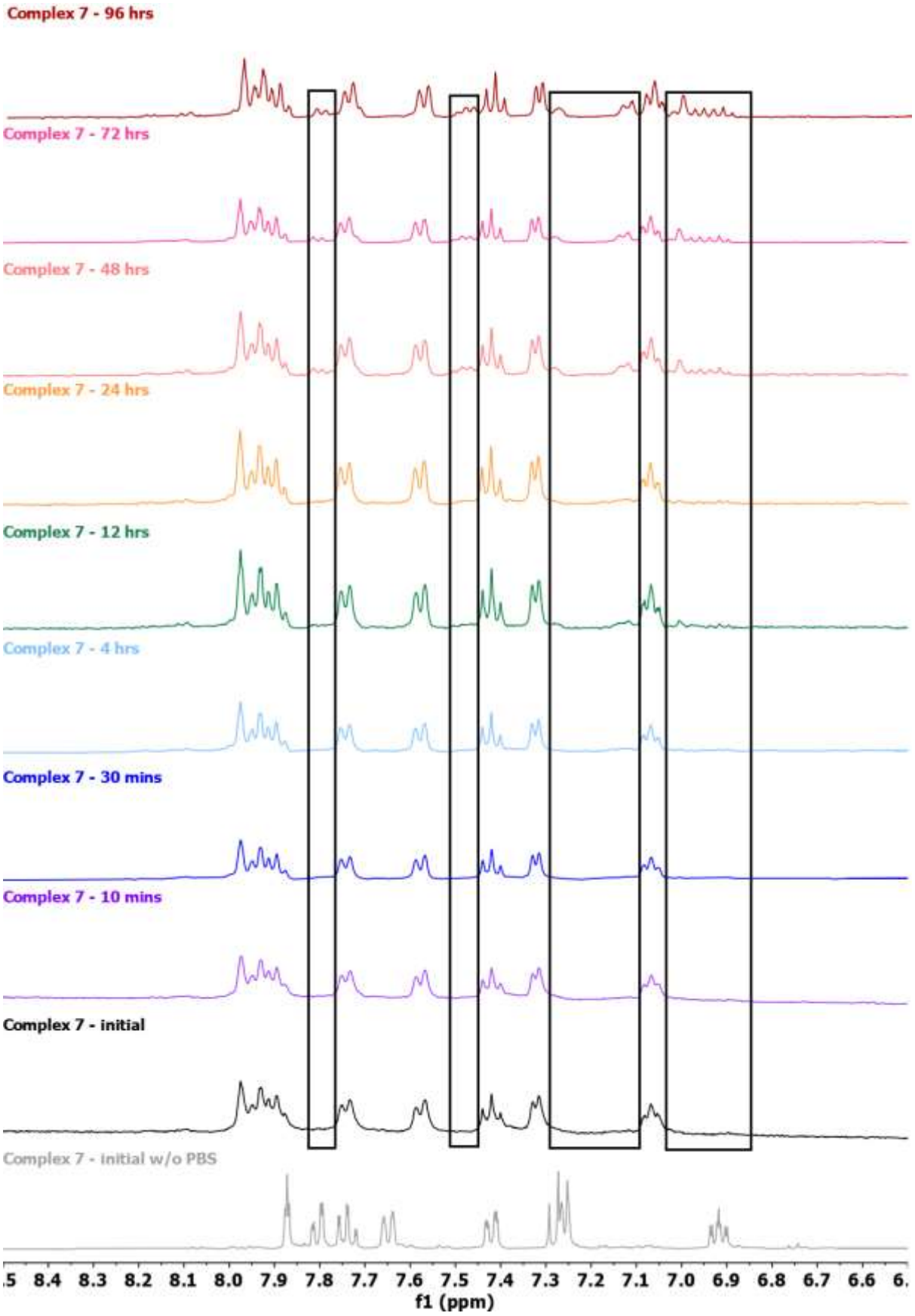

Figure S 15 Stability study of complex **7** in MeCN:PBS (80:20 *v/v*) over 96 h (d_3-MeCN, 300 K, 400 MHz).

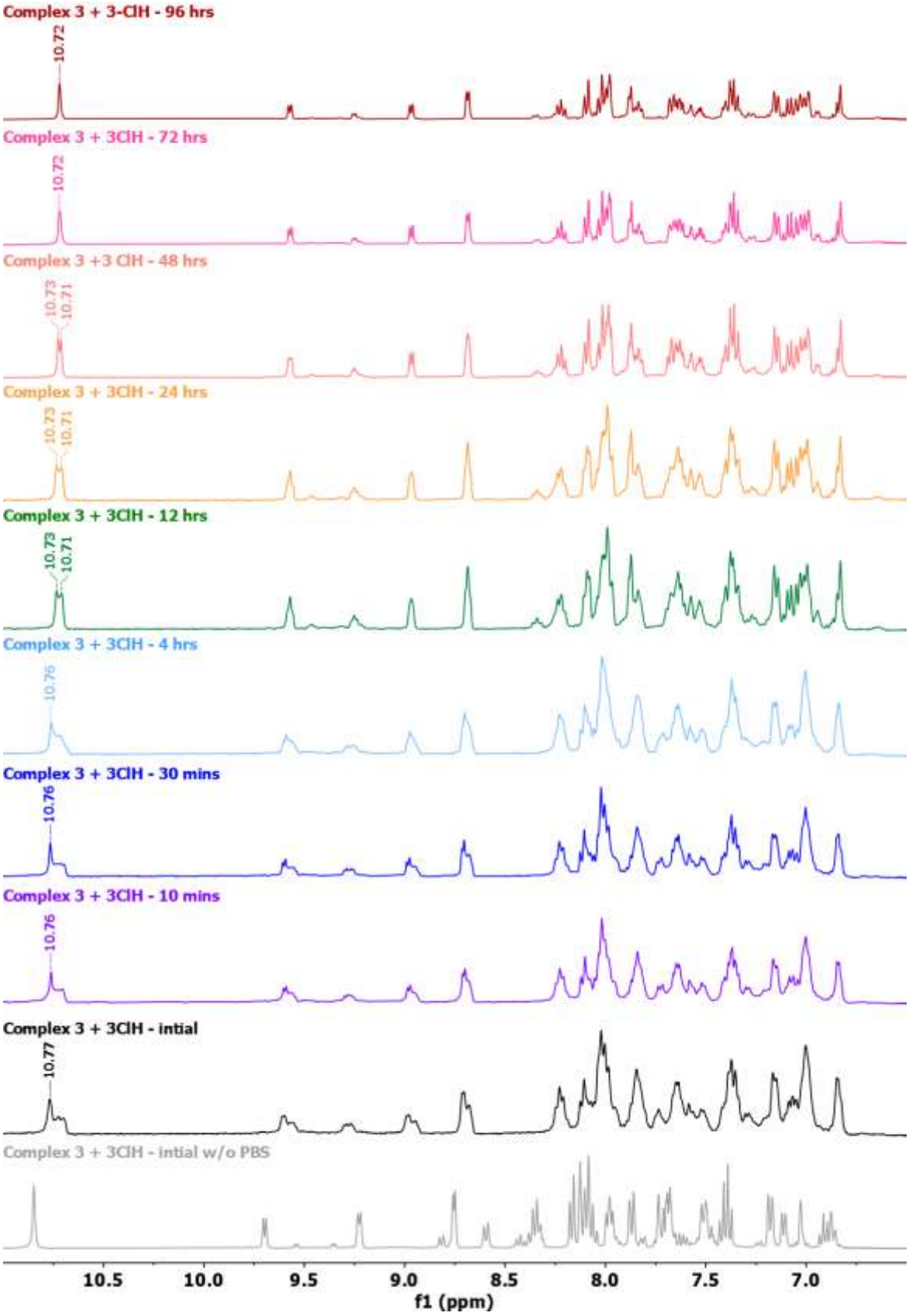

Figure S 16 Exchange studies of complex **3** with *N*-(3-chlorophenyl)picolinamide ligand (**L'**) in DMSO:PBS (80:20 *v/v*) over 96 h (d_6-DMSO, 300 K, 400 MHz).

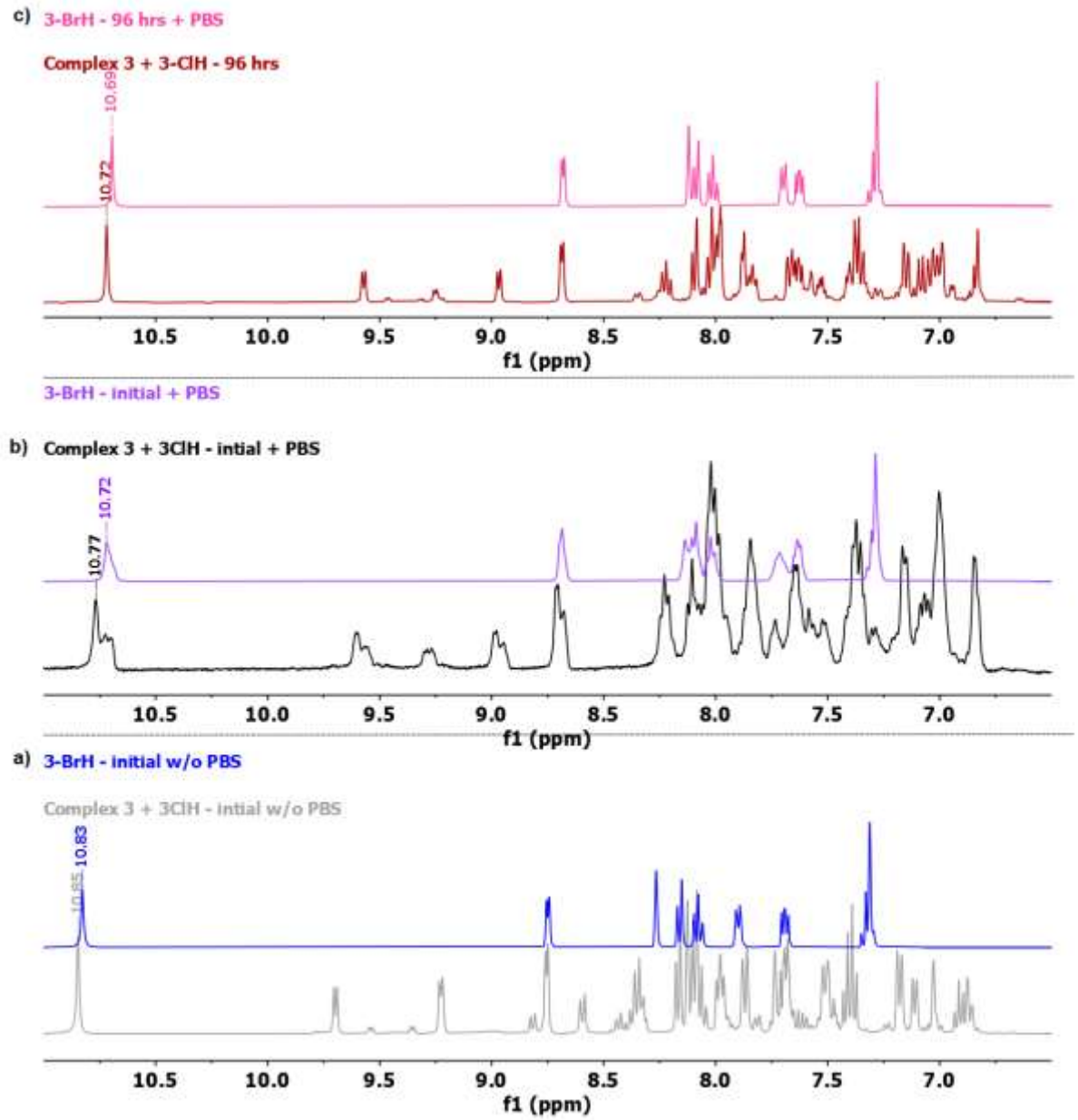

Figure S 17 Overlay of complex **3** and 3'-BrH in MeCN a) without PBS, b) with PBS (80:20 v/v) after initial and c) with PBS (80:20 v/v) after 96 h (d_3-MeCN, 300 K, 400 MHz).

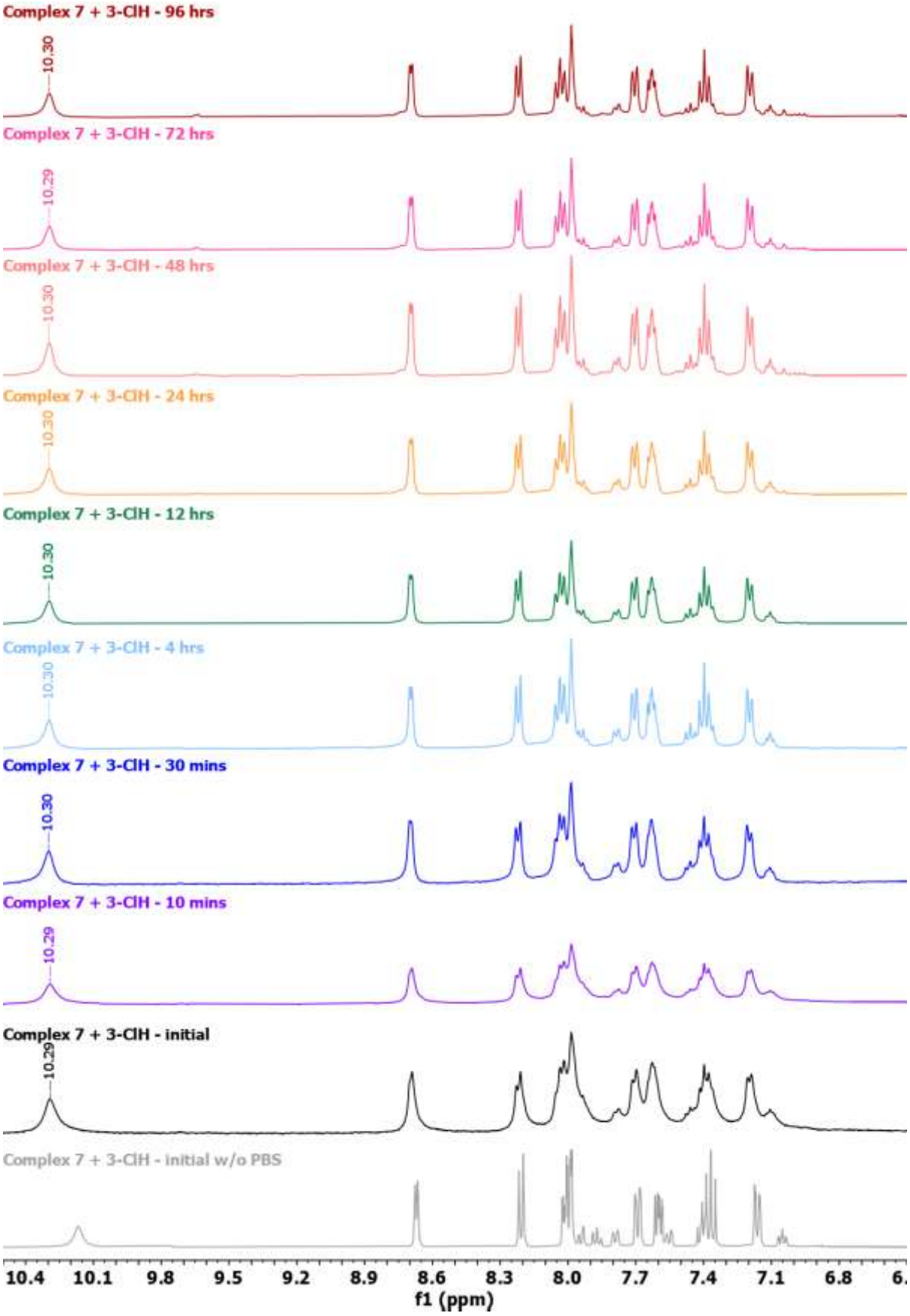

Figure S 18 Exchange studies of complex **7** with *N*-(3-chlorophenyl)picolinamide ligand (**L'**) in MeCN:PBS (80:20 *v/v*) over 96 h (d_3-MeCN, 300 K, 400 MHz).

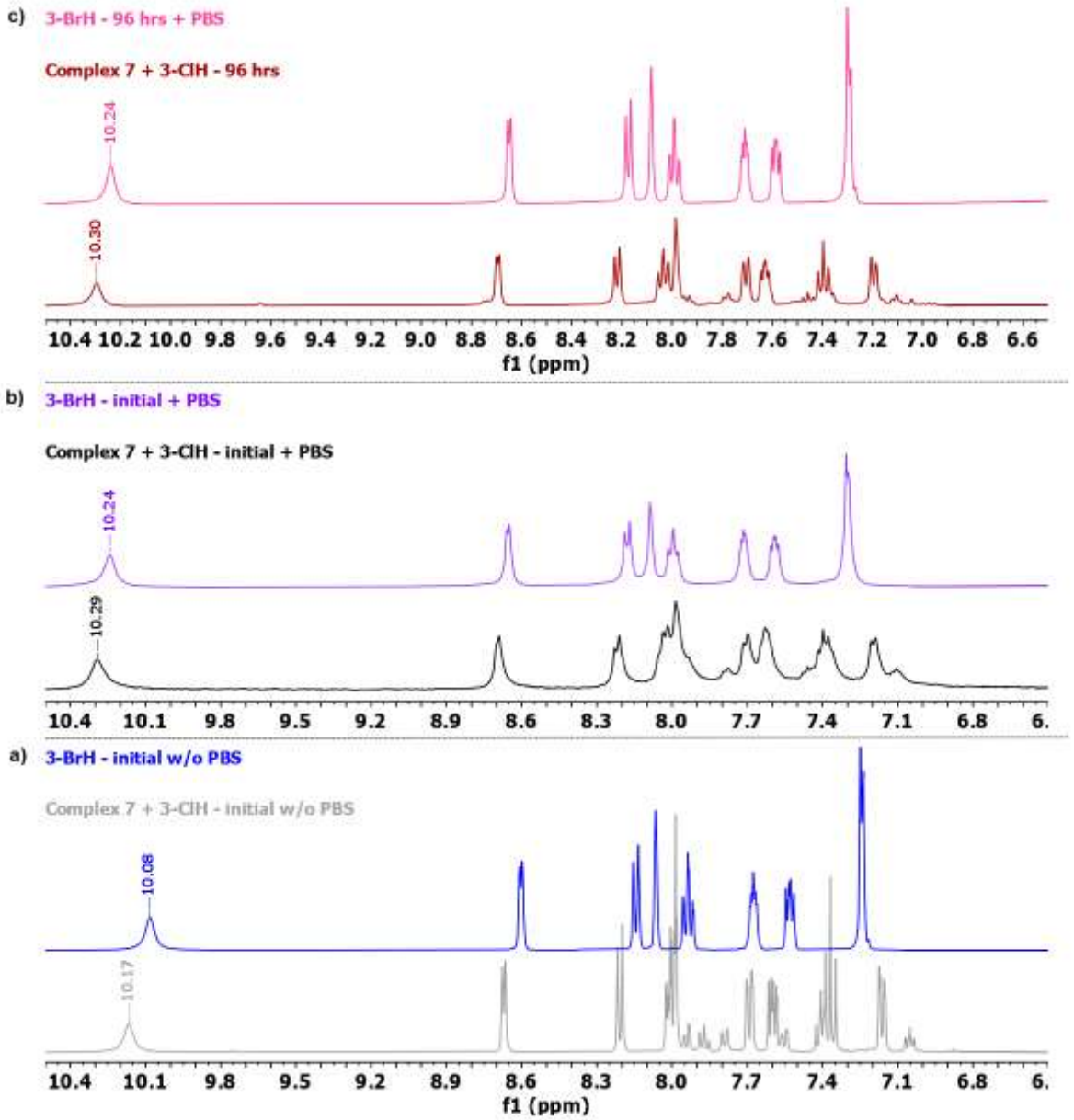

Figure S 19 Overlay of complex **7** and 3'-BrH in MeCN a) without PBS, b) with PBS (80:20 v/v) after initial and c) with PBS (80:20 v/v) after 96 h (d_3-MeCN, 300 K, 400 MHz).

96 h Chemosensitivity Studies

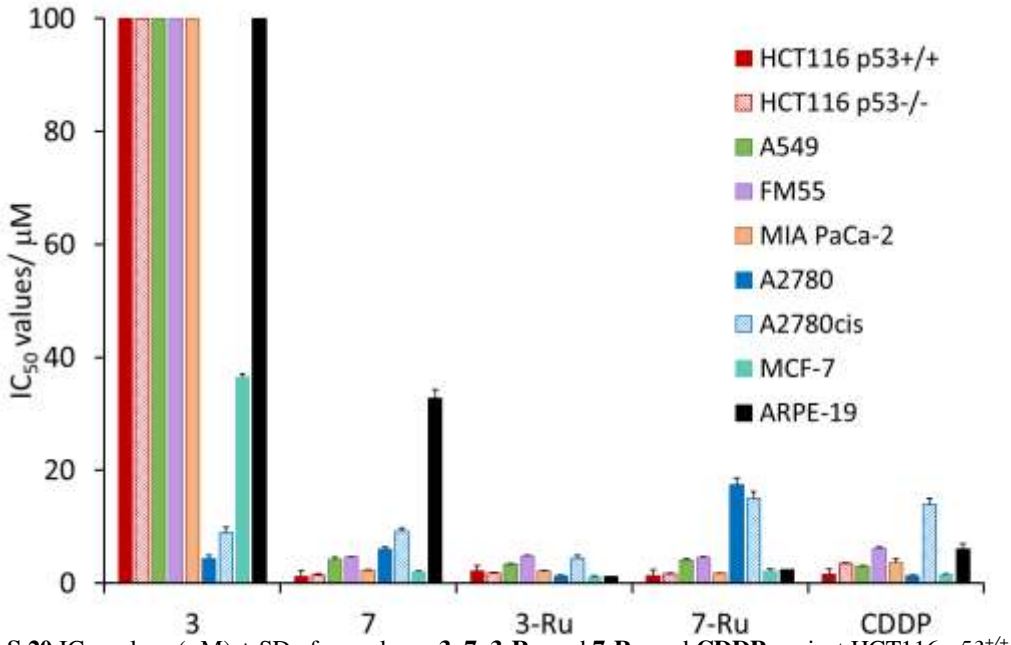

Figure S 20 IC_{50} values (µM) ± SD of complexes **3**, **7**, **3-Ru** and **7-Ru** and **CDDP** against HCT116 *p53*$^{+/+}$, HCT116 *p53*$^{-/-}$, A549, FM55, MIA PaCa-2, A2780, A2780cisR, MCF-7 and ARPE-19.

24 and 72 h Chemosensitivity Studies

Table S 5 IC_{50} values (µM) ± SD for complexes **3**, **7**, **3-Ru**, **7-Ru** and **CDDP** against HCT116 *p53*$^{+/+}$, HCT116 *p53*$^{-/-}$, and ARPE-19, after 24 h and 72 h incubation periods.

Complexes	IC_{50} values (µM) ± SD					
	HCT116 *p53*$^{+/+}$		HCT116 *p53*$^{-/-}$		ARPE-19	
	24 h	72 h	24 h	72 h	24 h	72 h
3	>100	>100	>100	>100	>100	>100
7	1.7 ± 0.1 (21.8)	1.33 ± 0.08 (27.8)	>100 (< 0.4)	>100 (< 0.4)	37 ± 1	33 ± 1
3-Ru	2.1 ± 0.2 (1.1)	2.02 ± 0.08 (1.2)	2.3 ± 0.2 (1.0)	2.10 ± 0.09 (1.1)	2.41 ± 0.07	2.2 ± 0.3
7-Ru	1.7 ± 0.1 (1.6)	1.29 ± 0.05 (2.1)	4.3 ± 0.1 (0.6)	4.07 ± 0.07 (0.7)	2.7 ± 0.2	2.5 ± 0.3
CDDP	77 ± 2 (0.5)	71.6 ± 0.4 (0.6)	>100 (< 0.4)	>100 (< 0.4)	41 ± 1	37 ± 1

Selectivity Factors (SF)

Table S 6 Selectivity Factors (SF) for complexes **7**, **3-Ru**, **7-Ru** and **CDDP** when comparing the IC_{50} values of the isogenic colorectal cancer cell lines (HCT116 $p53^{+/+}$ and HCT116 $p53^{-/-}$) after 24, 72 and 96 h incubation periods.

Complexes	SF towards HCT116 $p53^{-/-}$			SF towards HCT116 p53+/+		
	24 h	72 h	96 h	24 h	72 h	96 h
7	0.02	0.01	0.90	57.47	75.16	1.11
3-Ru	0.92	0.96	1.20	1.09	1.04	0.83
7-Ru	0.38	0.32	0.80	2.61	3.16	1.26
CDDP	0.77	0.72	0.42	1.30	1.40	2.36

LogP, Solubility and Pharmacokinetics

Table S 7 Predictions of logP, solubility and pharmacokinetics for complexes 1-8, 3-Ru and 7-Ru, using Swiss ADME.[1]

Complex	Log P (MLOG)	LogS (ESOL)	Solubility mg/ mL	Class	GI absorption	Pharmacokinetics
1	3.54	-8.33	$2.83x10^{6}$	Poorly soluble	High	P-gp substrate, CYP1A2 inhibitor, CYP2C19 inhibitor
2	3.91	-8.75	$1.16x10^{6}$	Poorly soluble	High	BBB permeant, P-gp substrate, CYP3A4 inhibitor
3	4.10	-9.38	$3.07x10^{7}$	Poorly soluble	High	BBB permeant, P-gp substrate
4	4.29	-9.91	$1.02x10^{7}$	Poorly soluble	High	BBB permeant, P-gp substrate
5	4.10	-9.09	$6.48x10^{7}$	Poorly soluble	High	BBB permeant, P-gp substrate
6	4.29	-9.96	$9.19x10^{8}$	Poorly soluble	High	BBB permeant, P-gp substrate
7	4.48	-10.59	$2.38x10^{8}$	Insoluble	High	P-gp substrate
8	4.67	-11.12	$7.66x10^{9}$	Insoluble	High	BBB permeant, P-gp substrate
3-Ru	4.10	-9.37	$3.15x10^{7}$	Poorly soluble	High	BBB permeant, P-gp substrate
7-Ru	4.48	-10.58	$2.43x10^{8}$	Insoluble	Hugh	P-gp substrate

References

(1) Daina, A.; Michielin, O.; Zoete, V. SwissADME: A Free Web Tool to Evaluate Pharmacokinetics, Drug-Likeness and Medicinal Chemistry Friendliness of Small Molecules. *Sci Rep* **2017**, *7* (Article number: 42717). https://doi.org/10.1038/srep42717.